Orbital
The electronic journal of chemistry

the electronic journal of chemistry

Full Paper | http://dx.doi.org/10.17807/orbital.v17i2.20480

Biosorption of Antimony Species by Red Macroalgae (Nori) and Cyanobacteria (*Spirulina*)

Vanessa Egéa dos Anjos* [a], Renata Martins da Silva [a], and Adriano Gonçalves Viana [a]

A biotechnological study with the *Porphyra tenera* (red macroalgae, "Nori") and *Spirulina platensis* (cyanobacteria) was performed to evaluate the feasibility of non-living biomass as biosorbent for inorganic antimony species to be used in the remediation technology or as solid phase for analytical purposes such as preconcentration. The biosorption of Sb(III) and Sb(V) was studied using batch technique under similar conditions of the aquatic environments. High values of biosorption (over 70%) of both Sb species were determined and factors such as dosage of the biomass, contact time and pH, practically did not influenced in the sorption. The desorption was evaluated using different concentrations of HCl and HNO_3. The biosorbents were characterized by X-ray diffraction, scanning electron microscopy (SEM), infrared spectroscopy (FTIR), surface area (BET) and zeta potential. The FTIR analysis after biosorption of the Sb species suggested the involvement of protonated functional groups as amino, carboxyl, and hydroxyl in the interaction mechanism. Thus, both biosorbents are suitable biosorption of Sb from aqueous solution.

Graphical abstract

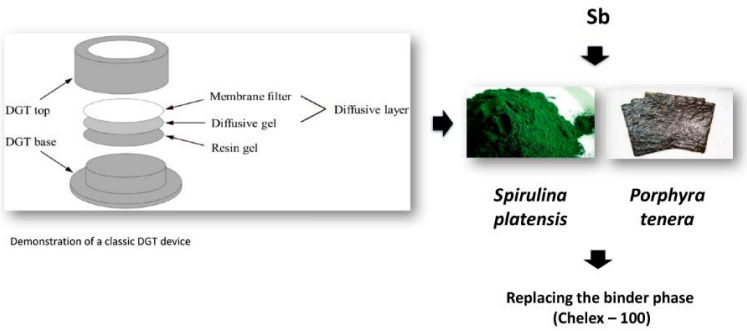

Keywords

Biosorption
Cyanobacteria
Porphyra tenera
Spirulina platensis
Sb(V)
Sb(III)

Article history

Received 24 Mar 2024
Revised 01 Jul 2024
Accepted 25 Mar 2025
Available online 17 May 2025

Handling Editor: Sergio R. Lazaro

1. Introduction

Antimony is a toxic metalloid present in the environment because of natural sources and anthropogenic activities [1-5]. Sb concentrations have been increasing, because Sb compounds are extensively used in flame retardants, batteries, metal alloy, catalyst, medication agent, manufacture of plastics, textiles, glass, semiconductors, etc. [2,5-9]. Thus, Sb has been declared as global contaminant. European Union and United States Environmental Protection Agency listed Sb as a priority pollutant [2-3, 9].

The behavior, distribution in the environmental, and toxicity of antimony and its compounds has become a worldwide concern [4,10]. These aspects are strongly dependent on its forms and chemical species (speciation). In aquatic environments, Sb is present in inorganic and organic

Departamento de Química da Universidade Estadual de Ponta Grossa (UEPG). Av. General Carlos Cavalcanti - Uvaranas, CEP 84030-900, Ponta Grossa, Paraná, Brasil. *Corresponding author. E-mail: **veanjos@uepg.br**

forms and in a variety of oxidation states. Species in inorganic form are known to be generally more toxic than organic forms [1,11-12]. Biogeochemistry behavior of antimony in surface waters is affected by environmental factors such as pH, redox conditions, presence of organic matter, clays minerals and biota [4]. Inorganic antimony might be found in nature in different forms. The two common inorganic forms present in natural waters are the trivalent form (antimonites - [Sb(III)]), and the pentavalent (+V) (antimonate - [Sb(V)]) [1-2, 13-15]. When comparing the inorganic forms, Sb(III) shows higher toxicity than Sb(V) [8].

In unpolluted natural waters, the Sb concentrations is very low, ranging from approximately ng L^{-1} to a few µg L^{-1}. However, there are many sources of Sb contamination that increase its concentration in the environment [8,16,17]. Sb is a non-essential element, a proven carcinogen agent and due its toxicity and non-biodegradable nature the determination of antimony in the environmental samples, as well as the development of technologies for removal from contaminated water are of interest.

Treatment methods (remediation) for antimony in natural waters include electrochemical, redox, ion exchange, extraction, membrane separation, coagulation, sedimentation, adsorption, phytoremediation and biosorption [4-5,18]. Adsorption is considered a suitable method because of their high efficiency and low cost. Many materials have been studied as sorbents for antimony species. The new trend is to search for new sorbents and in this context, biosorbents stands out due to its environmentally friendly advantages, simplicity, and efficiency [5,18-19]. In addition to the proposal to use biosorption as a remediation technique, the use of biosorbents can also be indicated in analytical methods. The determination of antimony in the environmental samples, is often an analytical challenge. Generally, extraction techniques can be used to separate, preconcentrate and determine one or more species of elements employing appropriate analytical techniques. Nowadays, solid phase extraction methods (SPE) based on the use of extractors in agreement with green chemistry concepts such as biosorbents are of interest [20-22]. Diffusive gradients in thin films (DGT) technique for speciation of trace elements in environmental samples employs a device that contains a binding phase (usually a chelating resin, Chelex-100). For Sb, it is necessary to use other types of solid phase for retention and preconcentration.

Biosorption describe the interaction of metallic species in aqueous solution through their binding to a biomass (living microorganisms or non-living) [18]. The typical biomasses are agricultural and plant waste, algae and microbial biomasses [5]. These materials have advantages such as the fact that they are natural, low cost, high efficiency, and can be used in the raw form or modified and show potential for reuse [23-25].

The mechanisms responsible for the biosorption of the metals and metalloids is complex and includes several processes such as electrostatic interaction, ion-exchange, complexation, microprecipitation, chemisorption, adsorption-complexation on the surface and in pores, surface adsorption, among others [18, 21,26-28]. However, the knowledge about antimony biosorption is still limited for all types of biosorbents [5, 8].

Biosorbents such as algal, bacteria, fungi, yeast have been studied for remediation of metals and metalloids in the natural waters. Among biosorbents, studies indicate that algal biomass contains many functional groups (carboxyl, amino, hydroxyl, sulphate, etc) that act as binding sites, which makes it have adequate sorption performance. Amino, carboxyl and hydroxyl groups are the mainly adsorption sites of Sb [4,29].

Several studies with cyanobacteria, known as blue-green algae, showed that it is a promising biosorbent due to its similarity with algae, presenting large surface area, being cheap, and produced for several commercial uses. Cyanobacteria are photosynthetic prokaryotes commonly found in natural environments. *Spirulina platensis* can remove metal ions from aqueous solutions [30-39]. Marine macroalgae (seaweeds) are alternative biomass materials for sequestering toxic metals [30,39-41]. However, studies with the red macroalgae *Porphyra tenera* as raw biosorbents are relatively scarce. Son et al. (2012) described that *Porphyra* is a commercially source of foods and drugs and an important model for algal research [42]. *Porphyra* is popularly known as "Nori" and is used in the preparation of sushi and commercialized as dried sheets.

Considering these aspects, this study aimed to investigate the red macroalgae, *Porphyra tenera* (for first time), and a cyanobacteria, *Spirulina platensis,* as potential biosorbent materials for Sb in aqueous solutions. The biomaterials were studied under experimental conditions different in the sorption of Sb(III) and Sb(V) that included biosorbent concentration, pH, time, Sb concentrations, etc. Desorption experiments using different eluents for antimony species were investigated to propose an application for biosorbents such as pre-concentrator material or use in the DGT devices. In addition, several analytical techniques were used for the characterization of both biosorbents and to investigate the mechanism of interaction with antimony.

2. Results and Discussion

Acid treatment and characterization of biosorbents

Biosorption is described as the process of sorption of soluble metals by microbial non-living biomass. The biosorption behavior of the non-living biomass depends on surface properties. Thus, various kinds of pre-treatment can be performed to obtain modifications on the surface of the biomaterials and increase their efficiency [18]. Initially, the morphological and elemental analysis of raw biosorbents (red macroalgae and cyanobacteria) were determined by SEM imagens and Energy Dispersive Microanalysis (EDS).

SEM-EDS analyses of biomasses showed that the main constituents were C and O. The percentages of C, O, Cl, and Na were 48.4%, 44.8%, 1.9%, 1.08% for macroalgae and 68.7%, 26.4%, 0.13% and 0.72% for cyanobacteria, respectively. In addition, both biomasses naturally have in their composition other trace elements, such as Sb, because they are in natura materials without previous treatment. The Sb percentage in samples were 17% and 5% for seaweed and cyanobacteria, respectively. This fact may indicate that the materials can interact with antimony species. Thus, it was necessary to perform an acid pretreatment with 0.5 mol L^{-1} HNO_3 for biomass decontamination. After, the Sb concentration was determined by GF AAS in the treated samples. For this purpose, the samples were kept in aqueous and acidic solution for 24h and the extracted Sb contents were below the limit of detection of the technique (1.0 µg L^{-1}) for both materials.

The morphology and structural aspects of the biomasses in natura and after acid treatment were analyzed by SEM-FEG (Fig. 1).

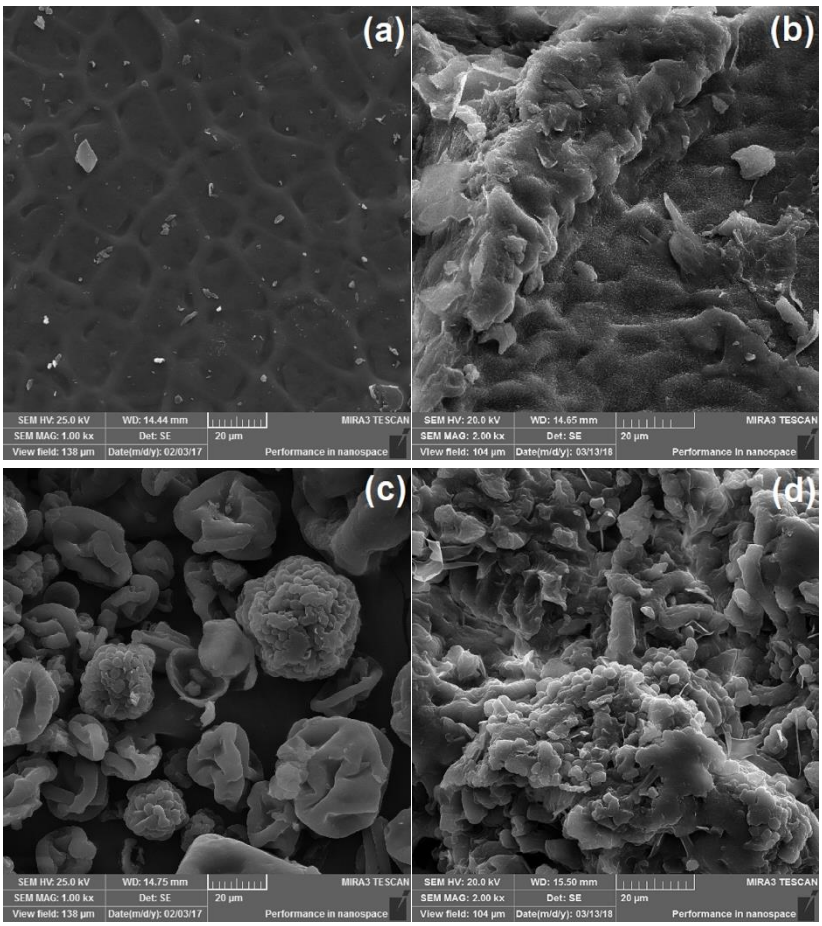

Fig.1. SEM-FEG photomicrographs of the *in natura Porphyra tenera* (a), treated *Porphyra tenera* (b), *in natura Spirula platensis* (c) and treated *Spirula platensis* (d). [SEM a-c: 1kx magnification]. [SEM c-d: 2kx magnification].

The SEM images of the alga *Porphyra tenera* in its natural state (Fig. 1a) revealed a thin film-like structure, with the presence of pores suggested by the photomicrographs. This was confirmed by BET measurements. Following acid treatment, the morphological structure of the alga (Fig. 1b) showed modifications, indicating an increase in roughness. Fig. 1c revealed spherical clustered structures for *in natura Spirulina platensis*. Expected images for Spirulina platensis obtained by SEM-FEG are filaments with a spiral shape [44-45]. This cyanobacterium is composed of cylindrical cells arranged in helical filaments [46-47]. In this work, the biomass structures observed may be due to the process for obtaining the dry powder biomass [48]. Fig. 1d showed that the acid treatment promoted a disruptive structure of the spheres for cyanobacteria biomass, increasing the roughness and obtaining irregular pores on the surface.

To identify the crystalline or amorphous phases, XRD measurements were performed (Fig. 2).

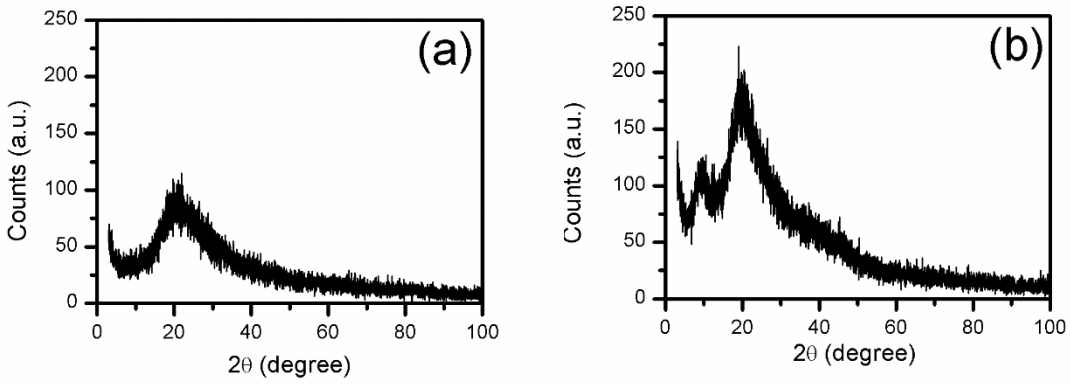

Fig. 2. X-ray diffractograms for in natura *Porphyra tenera* (a), and *Spirula platensis* (b).

Fig.2a showed the XRD pattern of *in natura Phorphyra tenera* and there was a board shape at 2θ values of 20.08º, indicating amorphous structure. Amorphous structures, also called vitreous structures, are formed by random atomic arrangements and without symmetry or long-range ordering. For *in natura Spirulina* (Fig.2b) broadening of peaks at 2θ values of 9.54º, 19.64º, and 45.93º was observed. These values were like those reported by Gunasundari and Kumar (2017) for *Spirulina platensis* which are 9,549°, 19,455°, and

46,033° corresponding to (111), (222), and (554) planes [49]. Those authors related that the structure is cubic and that the shape of diffractogram showed crystallinity of biomass and the broad peaks is due to a smaller particle size. However, in general, the amorphous structure observed for both biomasses may be related to the predominant hemicellulose and less cellulosic composition of carbohydrates characteristic of algae and cyanobacteria [50].

Surface characteristics of biomasses and treated biomasses, such as surface area, pore volume, size pore, and Zeta potential, are shown in Table 1.

Table 1. Characteristic of *Porphyra tenera* and *Spirulina platensis* (*in natura* and after treatment): surface area, pore volume and size pore determined by BET and BJH methods and Zeta potential.

Samples	Specific surface area (m^2 g^{-1})	Pore Volume (mm^3 g^{-1})	Average Pore Radius (nm)	ζ (mV)
In natura *Porphyra*	0.87	3.2	7.5	-26 ± 4
Treated *Porphyra*	0.17	1.4	16.6	32 ± 14
In natura *Spirulina*	0.31	0.6	3.6	-29 ± 4
Treated *Spirulina*	0.04	0.8	40.4	10 ± 5

Regarding the red macroalgae samples, Table 1 showed that the acid treatment changed its characteristics in terms of surface charge, surface area and porosity. The specific surface area and pore volume decreased for the treated biosorbent, while pore size increased. For both materials, the pore radius was in the range of 2 nm and 50 nm, indicating the presence of mesopores [51]. The interaction of antimony species with biosorbents can be facilitated by the presence of larger pores, especially for the treated material, due to easy access. Several works described that the material larger surface area increases sorption capacity [52]. Although, the acidic treatment has changed the morphology and reduced the surface area and pore volume of the macroalgae. This could impact the sorption capacity for metallic species, depending on the process involved, be it electrostatic, ion exchange, chemical or physical sorption, complexation, etc. Zeta potential analysis indicated that the negative surface charge (ζ = -26 mV) was modified to positive surface charge (ζ = 32 mV) following acid treatment. This change is significant due to the neutral or anionic characteristics of antimony species.

The acid treatment also modified the characteristics of spirulina. The specific surface area decreased with acid treatment of cyanobacteria and pore volume and pore radius increased (Table 1). The pore radius values were lower than 50 nm, thus they were considered mesopores. The Zeta potential indicated that the biomass had a negative charge (ζ = -29 mV) on the surface and after treatment, the surface has a positive charge (ζ = 10 mV).

When comparing the two treated biosorbents, it was observed that the Nori macroalgae has a larger surface area and pore volume, along with a greater positive charge on its surface. A high Zeta potential value (+ 30 mV) is crucial for physicochemical stability [53]. With regard the influence of the pH on surface charge of the treated biosorbents, Zeta potential was performed in aqueous suspensions of the materials in the range from pH 4 to pH 8. The results indicated that the values of potential decreased as function of the pH increase, but the potential remained with positive values, indicating the predominance of positive charges on the surfaces. Zeta potential ranged from 32 ± 13 mV to 20 ± 11 mV at pH range studied for *Porphyra tenera*. For *Spirulina platensis*, similar behavior was observed, and the Zeta potential was smaller than of the macroalgae, ranging from 9 ± 4 mV to 6± 4 mV.

The cell walls of macroalgae and cyanobacteria are similar, and they are composed of polysaccharides, proteins, and lipids with charged functional groups [8]. Fig. 3 shows the results obtained of the biomass characterization before and after acid treatment by FTIR for evaluation of the functional groups.

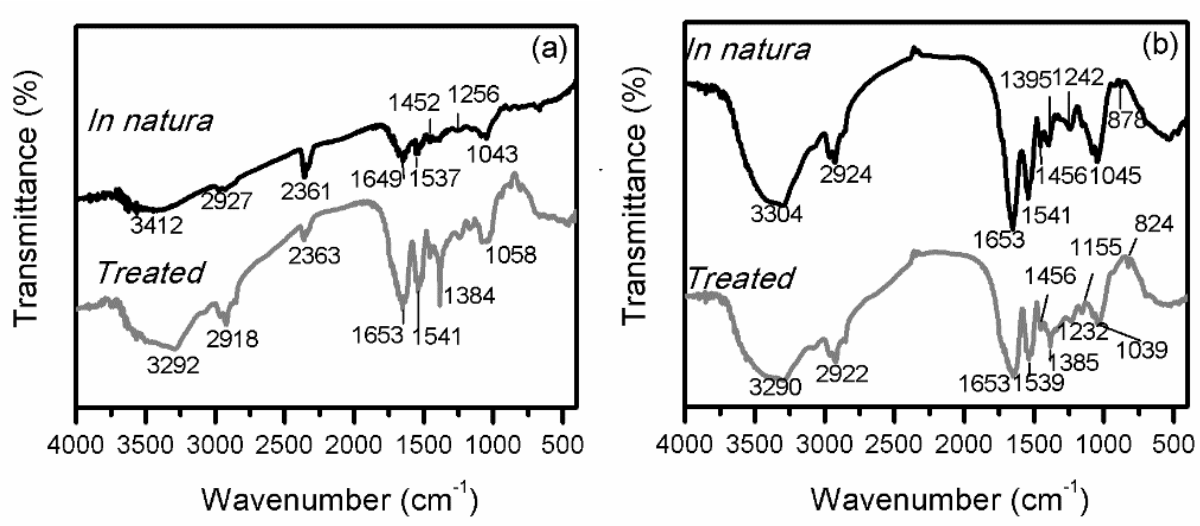

Fig. 3. FTIR spectra of *Porphyra tenera* (a), and *Spirulina platensis* (b).

The infrared spectrum for macroalgae *Porphyra tenera* (Fig. 3a) showed shifts of the bands when compared to the raw biomass and the treated biosorbent. Regarding raw and treated material, broad bands at 3412 and 3292 cm^{-1}, respectively, were assigned to the O-H and N-H stretching vibrations of groups, which are associated with the glucose present in the cell wall, and proteins and polysaccharides (carboxylic acid or amine). Bands observed at 2961 cm^{-1} corresponds to asymmetric stretching of CH_3 groups. Bands at 2918 and 2849 cm^{-1} could be assigned to asymmetric and symmetric stretching of CH_2 groups. The main bands centered at 1649, 1537 and 1452 cm^{-1} for *in natura* and at 1653, 1541 and 1456 cm^{-1} for treated algae, respectively, could be assigned to the C=O stretching vibration for amide and a combination of N-H binding of the amide bond of proteins. The band at 1256 and 1236 cm^{-1} for raw and treated biomass could be assigned to the C-O stretching vibration of the carboxylic group. C-N stretch vibration of the protein fraction was observed at 1043 and 1058 cm^{-1} for *in natura* and treated red macroalgae, respectively [40,56].

Fig. 3b shows the FTIR spectrum for cyanobacteria *Spirulina platensis* (*in natura* and treated). The biomass treated with acid solution present the same chemical composition as that of the raw material, because it was possible to observe the presence of the same bands, but with different intensity and shift. This fact can be related to the protonation of charged functional groups present in the biomass cell wall [57]. The spectra of raw and treated *Spirulina platensis* presented a broad band of N-H and O-H stretching vibrations at 3304 and 3290 cm^{-1}, respectively. Bands observed at 2963 and 2924 cm^{-1} for the *in natura* sample and bands at 2960 and 2922 cm^{-1} for treated sample were assigned to C-H asymmetric stretching modes of CH_3 and CH_2 groups. According to Wu et al. (2011), –CH stretching vibration of alkyl chains from fatty acid in membrane phospholipids in cyanobacteria can be observed at 2927 cm^{-1} [8]. The bands at 1653, 1541, and 1456 cm^{-1} for raw material and at 1653, 1539, and 1456 cm^{-1} for the treated material correspond to the binding of NH_2 group. Bands were observed at 1242 and 1045 cm^{-1} for the *in natura* sample and at 1232 and 1155 cm^{-1} for treated biosorbent indicating the C-N stretch of amide or amine groups. The bands at 878 and 824 cm^{-1} may be related to phosphatic groups in the raw and treated biosorbent, respectively [8, 53-56].

The characterization analysis performed in this work was important to determine the parameters (surface area, porosity, surface charge, functional groups, etc.) related to the biomass capacity and interaction mechanisms with metallic species. In addition, the results suggest that the acid treatment was important to remove impurities, increasing porosity and size pore, and the positive surface charge of the biosorbents due the protonation of charged functional groups present.

Effects of contact time, Sb concentration and biosorbent concentration on Sb(III) and Sb(V) biosorption

Studies were carried out to evaluate the most suitable experimental conditions: biomass dosage (Fig. 4), contact time (Fig. 5), and Sb concentration (Fig. 6) for sorption of Sb species onto treated biosorbents, taking into account the application of biomass as the solid phase in preconcentration systems or DGT devices, and the presence of Sb in natural waters.

Regarding the influence of biosorbent concentration in the biosorption, Fig. 4 shows that sorption percentages of Sb species did not depend on the amount of macroalgae and cyanobacteria, probably due to the porous characteristic and high availability of biding sites, according to the BET and FTIR analysis. Fig. 4a shows that the Sb(III) sorption ranged from 83 ± 4.8 % to 100 ± 8.2 % for *Porphyra tenera* and the Sb(V) sorption was maximum for the same biosorbent. *For Spirulina platensis*, Fig. 4b, the Sb(III) sorption ranged from 75 ± 8.4 % to 89 ± 6.7 % and Sb(V) sorption was maximum, respectively. In general, the biosorption of Sb(V) was higher than that of Sb(III) and there were no significant differences between the two biomass types in the biosorption of pentavalent species. For Sb(III), the biosorption onto red macroalgae was higher than that of cyanobacteria in the range of biomass dosage studied. This fact was attributed to the material larger surface area and pore volume (Table 1), providing more biosorption sites and functional groups for Sb(III). The choice of biosorbent dosage range is related to the literature and the minimum mass (0.3 g) of biosorbent needed to prepare a homogeneous hydrogel disc, with agarose and biosorbent, to be used in DGT devices as a binding phase. Peng et al. (2023) showed in the review work on adsorptive removal of antimony from waters that the dose of biosorbent used in some works varied from 0.5 to 50.0 g L^{-1} [5].

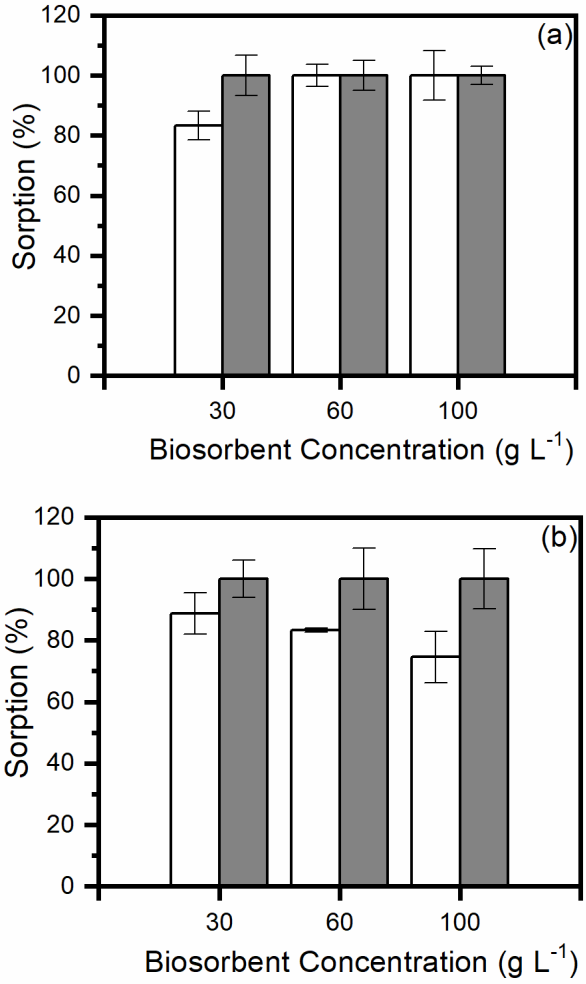

Fig. 4. Effect of biosorbent concentration on the sorption efficiency of Sb(III) (white) and Sb(V) (gray) for treated *Porphya tenera* (a) and *Spirulina platensis* (b). The bars represent the standard deviation (n=2). Initial Sb concentration: 15.0 µg L^{-1} and 1h as contact time.

The contact time in this experiment (Fig. 5) was 1h, but other works carry out studies with biosorption time from 0.5 to 240h [5]. The results obtained under the influence of time are shown in Fig. 5.

Fig. 5a shows that the contact time had little influence on Sb biosorption using treated biomass. The biosorption percentage was higher than 70% and can be considered appropriate. This behavior may be related to the biomass interaction mechanism. Normally, this step is fast and involves process on the surface of the dead biomaterial due to the presence of ligand groups in the cell wall [30]. In addition, in Fig. 5 the Sb(V) sorption was observed to be higher than Sb(III) for both materials. In general, there are no significant differences between the two biomasses in the sorption of antimony species for the estimated contact times. The Fig. 6 shows the influence of Sb concentrations on the biosorption.

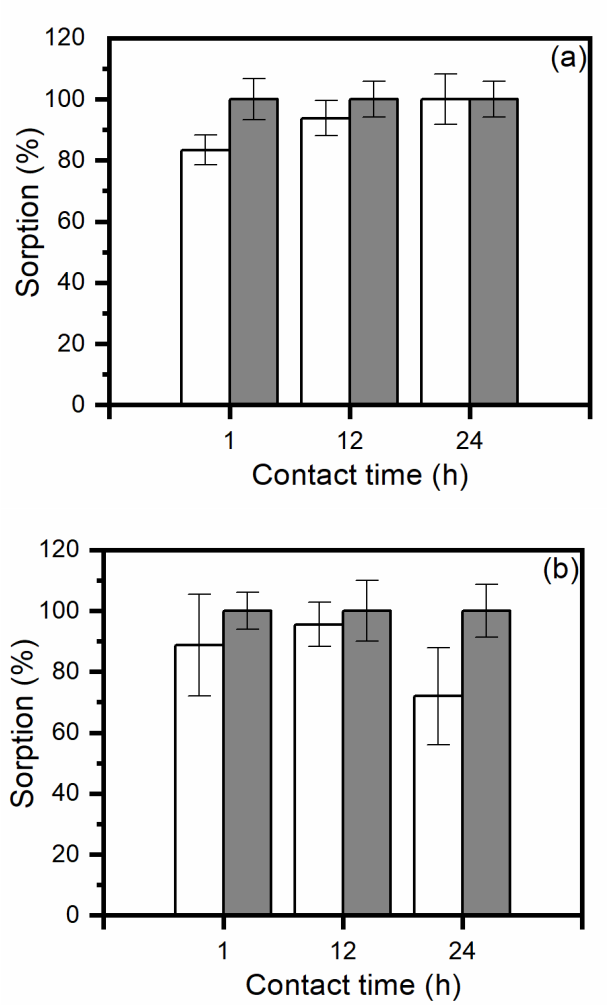

Fig.5. Effect of contact time on the sorption efficiency of Sb(III) (white) and Sb(V) (gray) for treated *Porphyra tenera* (a) and *Spirulina platensis* (b). The bars represent the standard deviation (n=2). Initial Sb concentration: 15.0 µg L^{-1} and biosorbents concentration: 30.0 g L^{-1}.

Fig. 6a shows that the Sb(III) sorption ranged from 42 ± 9.9 % to 100 ± 0.5 % and Sb(V) ranged from 80 ± 2 % to 97 ± 6.3 % for *Porphyra tenera*, respectively. Therefore, the Sb(V) sorption remains above 80% for the studied range. For Sb(III) it is observed that concentration above 30 µg L^{-1} there was a decrease in the percentage of sorption. This behavior may be related to the supersaturation of interaction sites for Nori for a longer interaction time. Regarding the *Spirulina platensis*, Fig. 6b shows that the sorption ranged from 59 ± 5 % to 97 ± 6.3% for Sb(III) and from 59 ± 4.7 % to 98 ± 2.4 % for Sb(V), respectively. The Sb(V) and Sb(III) sorption remains above 70%, except for the assay with 50 µg L^{-1} of initial concentration Sb species.

In general, it can be observed that both biosorbents treated with acid solution and with surface with positive charge interacted with the anionic species of antimony (trivalent and pentavalent). The biosorption percentages were adequate, regardless of the evaluated experimental conditions. Other experiments were performed with 30.0 g L^{-1} of treated biosorbents and 24h of contact time and 15 µg L^{-1} of the initial Sb concentration to minimize cost (amount of material) and chemical equilibrium conditions.

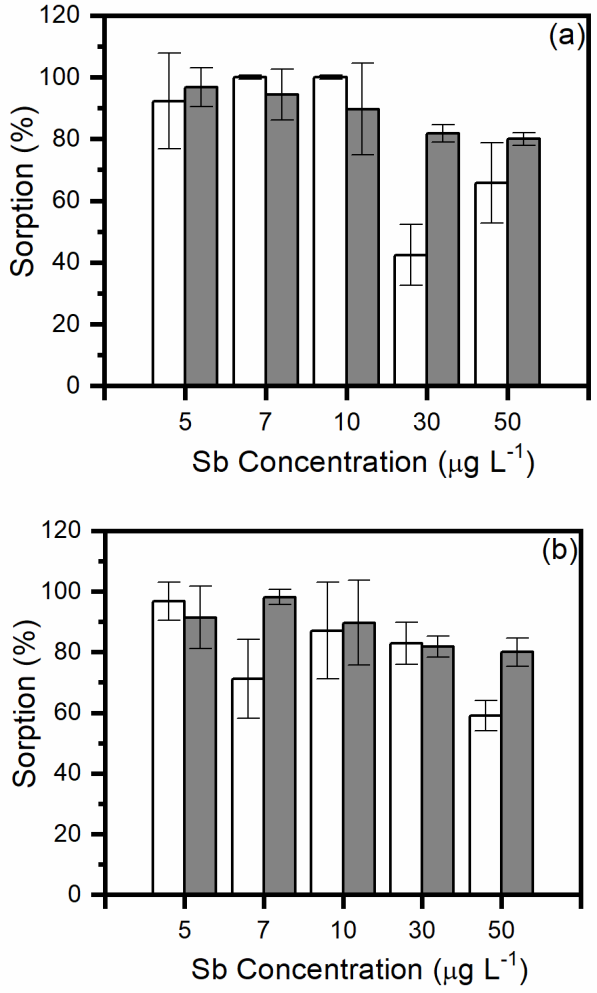

Fig. 6. Effect of Sb concentration on the sorption efficiency of Sb(III) (white) and Sb(V) (gray) for treated *Porphya tenera* (a) and *Spirulina platensis* (b). The bars represent the standard deviation (n=2). Contact time: 24h and biosorbents concentration: 30.0 g L^{-1}.

Influence of pH in the Sb biosorption

pH is an important parameter that can influence biosoprtion process, since it affects the element (Sb) speciation and the charge of functional groups on the biomass surface. Fig.7 shows the biosorption percentage of Sb(III) and Sb(V) onto *Porphyra tenera* and *Spirulina platensis* as a function of the pH solution.

The general trend observed in Fig. 7 was that the sorption of Sb(III) and Sb(V) is not significantly influenced by pH for both biosorbents. The results in Fig. 7a indicated that Sb(III) and Sb(V) was removed from the solution by Porphyra macroalgae over the pH range studied. For *Spirulina plantensis*, Fig. 7b, the percentage biosorption of Sb(III) ranged from 58 ± 8% (pH 4) to 97 ± 3% (pH 8). The percentages of Sb(V) biosorbed varied between 76 ± 17% (pH 4) and 98 ± 4.9 % (pH 8). Thus, the results demonstrate that Sb species biosorption was high over the whole pH range studied, which is the range found in aquatic environments. This antimony behavior can be considered an advantage, since it is not necessary to adjust the pH, minimizing costs and analysis time.

The higher adsorbed amounts of Sb(III) and Sb(V) can be explained by the Sb speciation and the predominance of the positive surface charge as shown by Zeta potential of both treated biosorbent at pH 4-8. In this pH range, anionic species of Sb(V) such as $Sb(OH)_6^-$ and neutral species of Sb(III) such as $Sb(OH)_3$ are the thermodynamically stable states. The positive charge on the surface of the materials indicated the predominance of chemical groups in protonated form. Therefore, there is no electrostatic repulsion of the Sb species by the biosorption sites. The mechanism involved in the biosorption can be surface complexation by protonated groups in the biomass.

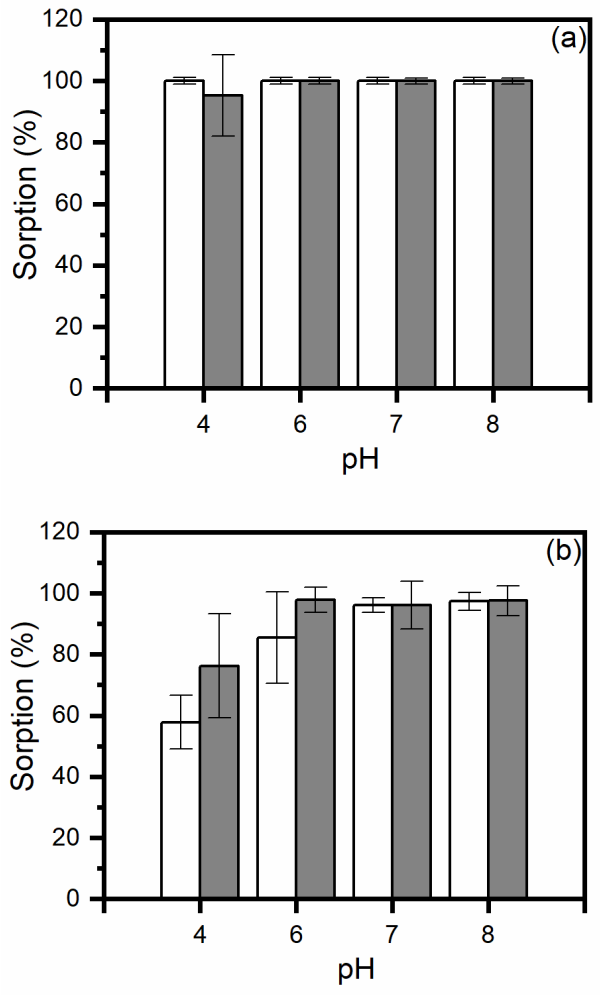

Fig. 7. Effect of pH on the sorption efficiency of Sb(III) (white) and Sb(V) (gray) for treated *Porphya tenera* (a) and *Spirulina platensis* (b). The bars represent the standard deviation (n=2). Initial Sb concentration was 15.0 μg L^{-1} and dosage biosorbents were 30.0 g L^{-1} of 24h after contact time.

Other studies reported similar results for the pH effect on sorption of antimony by biomass. Ungureanu et al. (2016) observed that Sb(III, V) uptake by green seaweed (*Cladophora sericea*) was strong over the wide pH range studied (pH 2-8) [59]. Wu et al (2012) reported that Sb adsorption was weakly pH dependent for pH in the range 2.0 – 7.0 for cyanobacteria Microcystis biomass [60].

Desorption experiments

Desorption of antimony from the biomass after sorption assays is important to determine the regeneration performance and usefulness of these biosorbents, especially in analytical and environmental applications such as binding phase in DGT devices. Desorption was evaluated using acid extractors in different concentrations (Fig. 8). Blanks were performed to check possible contamination.

According to Fig. 8a the desorption from macroalgae varied between 18 ± 0.1% (Sb(V)) using 6.0 mol L^{-1} HCl and 36 ± 22% (Sb(III)) using concentrated HCl. However, in general, when comparing the desorption values between the two extractors, no significant differences were observed. The same behavior was noted when comparing the desorption percentages using different concentrations of the same extractor. High values of standard deviation were obtained when using concentrated hydrochloric acid. This fact can be related to the interference in the measurements by GF AAS and a high value of background signal.

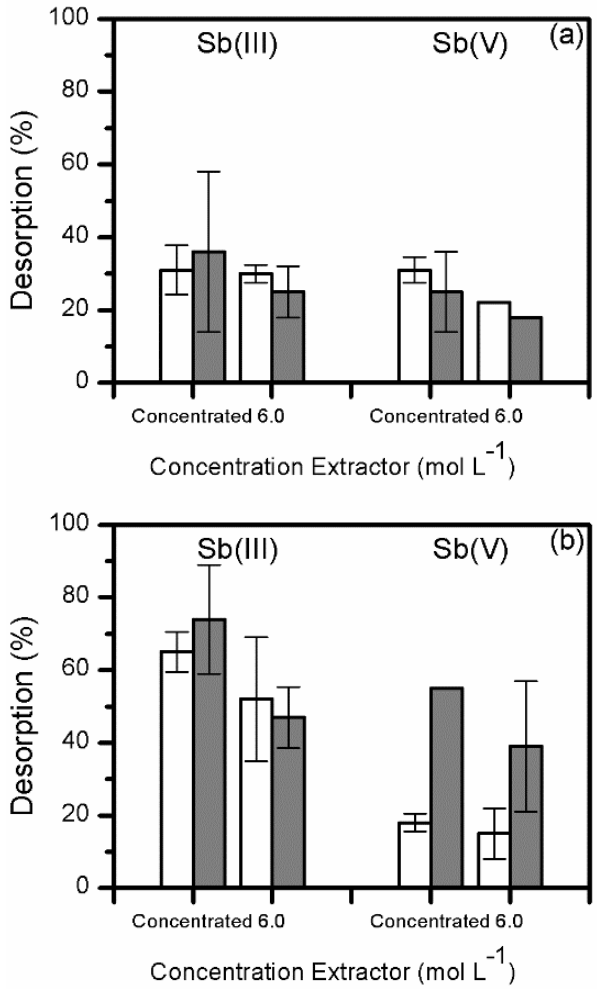

Fig. 8. Desorption of antimony from *Porphyra tenera* (a) and *Spirulina platensis* (b) using HNO_3 (white) and HCl (gray). The bars represent the standard deviation (n=3).

For *Spirulina* samples, the desorption percentage (Fig. 8b) ranged from 18 ± 24% (Sb (V)) using concentrated HNO_3 to 74 ± 15% (Sb(III)) using concentrated HCl. Desorption values for cyanobacteria were higher than values found for macroalgae, however an opposite behavior was observed for biosorption. Therefore, the greater the interaction of antimony with biomass, the lower the desorption capacity. The desorption process may depend on various factors, including the type of biomass, the characteristics of the element, the concentration and type of extractant, and the mechanism involved. The desorption mechanism is still not well studied in the literature. It may be related to ion exchange interactions and chemical sorption. Additionally, the protonation and deprotonation processes of the chemical groups involved, as well as the competition between the analyte and the H^+ ions, play a role in the desorption process.

The complete removal of antimony sorbed in the material was not possible using acid solutions. However, this is not necessarily due to the use of the correction factor (recovery factor) in the recovery calculations in the application of biomaterials as solid sorbent in the solid extraction methodology or DGT devices.

In general, HNO_3 can be considered an extractor for antimony onto both biosorbents, due to the lower standard deviation value, except for Sb(V) and *Spirulina platensis*. Wu et al. (2012) described that desorption efficiency was 63.1% using 4 mol L^{-1} of HCl for sorbed Sb(III) in the *Microcystis* biomass [60].

FTIR analysis in the sorption experiments

FTIR was used to study the mechanisms involved in the Sb biosorption based on the functional groups present in the acid treated biomass. The infrared spectrum of the acid treated biomass with and without Sb biosorption was analyzed. Fig. 9 shows the spectra obtained after sorption of Sb(V) and Sb(III) for *Porphyra tenera* and *Spirulina*. Fig. 3 shows FTIR spectra of biomass without Sb species.

The FTIR spectra of *Porphyra tenera* after Sb sorption (Fig. 9a) was compared to treated biomass (Fig. 3a). The shifts of bands positions can be related to biosorption. Thus, these changes may be indicative of the chemical groups that are involved in the biosorption process. The characteristic bands for the treated *Porphyra* biomass were observed in Fig. 3a at 3497-3292, 2918-2849, 1653, 1541, 1541-1456, 1236, 1165, 1058 cm^{-1}. After Sb(III) biosorption, the characteristic bands were seen at 3375-3294, 2926-2872, 1651, 1533-1450, 1238, 1159, 1080 cm^{-1}. After Sb(V) biosorption, the characteristic bands were noted at 3288-3074, 2922-2866, 1647, 1533-1458, 1232, 1169, 1066 cm^{-1}. The changes of band position in the region of 3475-3288 cm^{-1} suggest that N-H or O-H groups are involved in the Sb(III) and Sb(V) interaction. The band alteration at 1651-1647, 1533, 1456-1458 cm^{-1} indicating that amino and carboxyl groups (C=O and N-H) are important functional groups in the binding of Sb(III) and Sb(V). Groups C-O of carboxylic acids and C-N of proteins at 1159 and 1169, and 1080 and 1066 cm^{-1}, respectively, are also involved in the Sb(III) and Sb(V) sorption.

For *Spirulina* biomass, the raw biomass shifts of characteristic bands positions indicated that interactions of Sb(III) and Sb(V) with carboxyl, hydroxyl, amino and phosphatic groups were mainly responsible for the biosorption. The characteristic bands of the treated *Spirulina* (Fig. 3b) were observed at 3458, 2976-2927, 1651, 1539, 1456, 1385, 1155, 1040, 826 cm^{-1}. After Sb(III) biosorption (Fig. 9b), the characteristic bands were seen at 3437-3288, 2963-2918, 1649, 1542, 1456, 1384, 1240, 1155, 1045, 876 cm^{-1}. After Sb(V) biosorption (Fig. 9b), the characteristic bands were noticed at 3453, 2976-2922, 1651, 1539, 1454, 1384, 1155, 1045, 879 cm^{-1}.

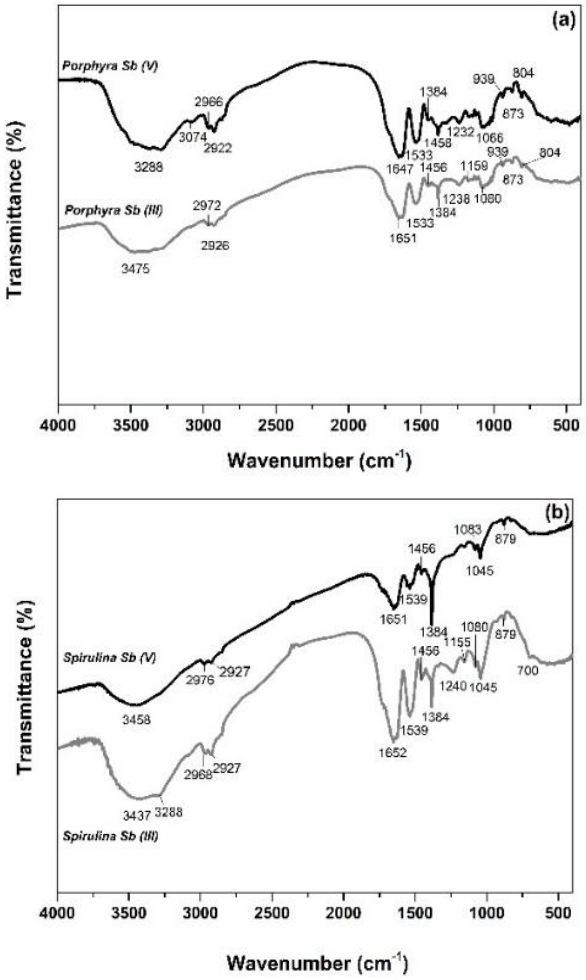

Fig. 9. Fourier transform infrared spectroscopy (FTIR) spectra: Comparison of FTIR spectra after sorption of Sb(III) and Sb(V) for *Porphyra tenera* (a) and *Spirulina* (b).

These results are similar to other studies with Sb and cyanobacteria Microcystis biomass [8,57]. Wu et al. (2012) described the complexation mechanisms of carboxyl and hydroxyl groups present on the cell wall of *Microcystis* with $Sb(OH)_3$ [60]. Sun et al. (2011) also reported the complexation mechanism of $Sb(OH)_6^-$ [29]. However, the full mechanism of interaction between antimony and chemical groups of the biosorbents is not fully understood.

In this study, the Zeta potential revealed the predominance of the positive charge in the treated biomass and FTIR studies were performed at pH 4. Thus, the protonated amine groups, as well as carboxyl and hydroxyl groups would provoke the interaction of anionic Sb(V) through electrostatic attraction and through the complexation with Sb(V). Regarding the neutral species, Sb(III), the interaction process may have resulted from the formation of surface complex among Sb(III) and protonated functional groups.

3. Material and Methods

Reagents and apparatus

All reagents used in this work were analytical grade or better. Ultrapure water was obtained from Milli-Q system (Millipore). Clean techniques were adopted, glassware and plastic material were acid-washed and rinsed with ultrapure water [22].

The working standard solutions of Sb(V) were prepared by dilution of individual 1000 mg L^{-1} standard solution of Sb (TraceCert - Sigma Aldrich). Analytical standard solutions were prepared by dissolution of Sb_2O_3 (Sigma Aldrich) in 2.0 mol L^{-1} HCl solution.

The determination of all antimony species was carried out using an atomic absorption spectrometer (AA 240 Z Varian, Agilent) equipped with Zeeman background correction and graphite tube atomizer (GT 120) linked to an auto-sampler (PSD 120). An antimony hollow cathode lamp (Varian, Agilent) was used as radiation source, operation at λ = 217.6; i = 10 MA, slit size = 0.2 nm. Argon was used as inert gas and pyrolytic graphite tubes were used. The pyrolysis and atomization temperatures used were 700 ºC and 2000 ºC, respectively. Background (BG) correction integrated absorbance of peak area was employed as the analytical signal. The quantifications were performed in triplicate (n=3) by external standardization. Analytical curves were used in the range of 1.0 to 30.0 µg L^{-1}.

The pH measurements were carried out using a potentiometer coupled to an Ag/AgCl combination glass electrode (Methrom, model 827 pH Lab). A centrifuge (80-2B Centrifuge), a stove (Nova Técnica) and an orbital shaker (SP 222, SPLabor) were used for the treatment of biosorbents and for the sorption and desorption studies.

The morphological characterization of biosorbents was performed using Scanning Electron Microscopy with Emission Source for Field Effect -FEG-SEM (TESCAN, model Mira 3) at various magnifications. In addition, a semi-quantitative microanalysis was performed by Dispersive Energy Spectroscopy - SEM-EDS.

X-ray Diffraction (XRD) measurements were carried out in a Rigaku diffractometer model Ultima IV, using Cu Kα radiation.

The Fourier Transformed Infrared (FTIR) spectra were recorded from 4000 to 400 cm^{-1} on an IR spectrophotometer with diffuse reflectance accessory (Shimadzu, IRPrestige-21, DRS-8000).

The N_2 adsorption isotherms were obtained using Quantachrome® Nova 1200e equipment. The specific surface area was calculated from the isotherms using a BET (Brunauer, Emmett and Teller) model. Pore sizes and volume were obtained employing BJH method (Barrett, Joyner, Helenda).

The Zeta Potential of the biosorbents were measured using a Zeta sizer analyzer (Nano Zs90) from Malvern.

Red macroalga and cyanobacteria biomasses and biosorbents preparation

The *Spirulina platensis* biomass was purchased in drugstore from Ponta Grossa, State of Paraná, Brazil. The *Porphyra tenera* samples were purchased in supermarkets from Ponta Grossa and Curitiba; State of Paraná, Brazil; as dried edible seaweed sheets. For one brand, products from different lots were used and a composite sample was used. Each dried biomass sample was reduced into small fragments and a quartering method was used to guarantee the homogeneity of the samples.

The samples of biomasses were individually treated with 0.5 mol L^{-1} HNO_3 for six times. After the acid treatment, the solids were washed with ultrapure water (three times) and centrifuged. The materials were dried at 50 ºC for 24h. To obtain powder, the biomasses were macerated with mortar and pistil and then sieved. After this procedure, the biosorbent were stored and used in biosorption tests and characterization assays.

Sorption studies for Sb species with biosorbents

All sorption studies were carried out as batch experiments in ambient conditions (room temperature) using known masses of the treated biomaterials and individual solutions of Sb(III) and Sb(V). The suspensions were shaken for in Falcon tubes. After the contact time, the suspensions were centrifuged at 2000 rpm and the supernatants were used in the determination, by GF AAS, of remaining concentration of Sb in solution. The concentration of each Sb specie sorbed on the biosorbents was calculated by difference between the initial concentration and the concentration in the supernatant. Blanks samples of the biosorbents were used as controls. All tests were performed in triplicate, and the results were expressed as mean values.

Some important paraments were studied (univariate mode) in the sorption experiments for each Sb species and each treated biosorbent. The chosen conditions were related to the applications of materials as adsorbent phases for analytical purposes and environmental remediation. Thus, the values of the parameters were related to the conditions normally found in aquatic environments. The influence of biomass concentration was studied using 30.0; 60.0 and 100.0 g L^{-1} concentrations of dry biosorbents. The concentrations of Sb ranged from 5.0 to 50.0 µg L^{-1}. The contact time was studied, and the values ranged from 1 h to 24h. The effect of pH on the sorption was investigated using Sb solutions at pH 4.0 until pH 8.0 was reached. The pH of the solutions and suspensions was adjusted with of 0.1 mol L^{-1} NaOH or 0.1 mol L^{-1} HNO_3 solutions.

Desorption studies

Experiments regarding the desorption of Sb(V) or Sb(III) from biosorbents were carried out. The solid phase obtained in the sorption studies was used in the desorption assays. Tests were performed with different eluents HNO_3 and HCl and a 24h extraction period. The concentrations of eluents used were 0.5, 1.0 and 6.0 mol L^{-1}. After centrifugation (2000 rpm), the supernatants were used in the determination of Sb by GF AAS.

FTIR studies

To understand the sorption process in the treated biosorbents, FTIR analysis were performed with treated biosorbents and biosorbents recovered at the end of sorption tests using 50.0 mg L^{-1}.

4. Conclusions

It was possible to conclude that treated biomass in powder form (*Porphyra tenera and Spiruluna platensis*) can produce good biosorbents for inorganic antimony species and they can be used in treatment systems in aquatic environments or as solid phase for extraction and preconcentration in analytical systems such as DGT devices.

The acid treated biosorbents exhibited high capacity of Sb sorption in a wide range of experimental conditions, such as biomass concentration, contact time, and pH. The biosorption assays were carried out under similar conditions as those of natural waters, especially in trace concentrations. The desorption of Sb species was evaluated with a single process using HNO_3 and HCl. The characterization of the biosorbents was important do understand the mechanism of interaction among biomaterials and analytes. The presence of protonated amine groups, as well as carboxyl and hydroxyl groups in the biomass was essential in the biosorption of Sb(III) and Sb(V) by complexation reactions and by electrostatic attraction and formation of the complex, respectively.

Acknowledgments

Authors are grateful to UEPG - State University of Ponta Grossa, C-LABMU / UEPG - Multiuser Laboratory Complex), CAPES - Coordination of Superior Level Staff Improvement and CNPq - National Council for Scientific and Technological Development (448270/2014-5) for financial support. In addition, thank State University of Londrina (UEL), especially Prof. Dr. César Ricardo Teixeira Tarley by surface area measurements.

Author Contributions

Vanessa Egéa dos Anjos: Conceptualization, funding acquisition, methodology, project administration, resources, supervison, writing – original draft and writing – review & editing. Renata Martins Silva: data curation, formal analysis, investigation, methodology, validation and writing – original draft. Adriano Gonçalves Viana: conceptualization, methodology, supersion and writing – review & editing

References and Notes

[1] Filella, M.; Belzile, N.; Chen Y. W. *Earth-Sci. Rev*. **2002**, *57*, 125. [Crossref]

[2] Li J.; Zheng, B.; He, Y.; Zhou Y.; Chen, X.; Ruan, S.; Yang, Y.; Dai, C.; Tang, L. *Environ. Saf.* **2018**, *156*,125. [Crossref]

[3] He, M.; Wang, N.; Long, X.; Zang, C.; Ma, C.; Zhong, Q.; Wang, A.; Wang, Y.; Pervaiz, A.; Shan, J. *J. Environ. Sci*. **2019**, *75*, 14. [Crossref]

[4] Zhang, Y.; Ding, C.; Gong, D.; Deng, Y.; Huang, Y.; Zheng, J.; Xiong, S.; Tang, R.; Wang, Y.; Su, L. *Environ. Technol. Innovation* **2021**, *24*,102026. [Crossref]

[5] Peng, L.; Wang, N.; Xiao, T.; Wang, J.; Quan, H.; Fu, C.; Kong, Q.; Zhang, X. *Chemosphere* **2023**, *327*,138529. [Crossref]

[6] Rath, S.; Trivelin, L. A.; Imbrunito, T. R.; Tomazela, D. M.; Jesús, M. N.; Marzal, P. C. *Quim. Nova* **2003**, *26*, 550. [Crossref]

[7] Foster, S.; Maher, W.; Krikowa, F.; Telford, K.; Ellwood, M. *Environ. Monit*. **2005**, *7*, 1214. [Crossref]

[8] Wu, H.; Wang, B.; Liu, Y.; Liu, S.; Li, J.; Lu, J.; Tian, W.; Zhao, Z.; Yang, Z. *Spectrochim. Acta, Part B* **2011**, *66*, 74. [Crossref]

[9] Andrade, M. da R.; Costa, J. A. V. *Cienc. Tecnol. Aliment*. **2008**, *32*, 1551. [Crossref]

[10] Amarasiriwardena, D.; Wu, F. *Microchem. J.* **2011**, *97*, 1. [Crossref]

[11] Larios, R.; Fernández-Martínez, R.; LeHecho, I.; Rucandio, I. *Sci. Total Environ*. **2012**, *414*, 600. [Crossref]

[12] Shakerian, F.; Dadfarnia, S.; Shabani, A. M. H.; Abadi, M. N. A. *Food Chem*. **2014**, *145*, 571. [Crossref]

[13] Accornero, M.; Marini. L.; Lelli, M. *J. Solution Chem*. **2008**, *37*, 785. [Crossref]

[14] Hockmann, K.; Lenz, M.; Tandy, S.; Nachtegaal, M.; Janousch, M.; Schulin, R. *J. Hazard Mater*. **2014**, *275*, 215. [Crossref]

[15] Ilgen, A. G.; Majs, F.; Barker, A. J.; Douglas, T. A.; Trainor, T. P. *Geochim. Cosmochim. Acta* **2014**, *132*, 16. [Crossref]

[16] Fu, X.; Xie, X.; Charlet, L.; He, J. *J. Hydrol*. **2023**, *625 Part* B, 130043. [Crossref]

[17] Ungureanu, G.; Santos, S.; Boaventura, R.; Botelho, C. *J. Environ. Sci*. **2015**, *151*, 326. [Crossref]

[18] Prya, A. K.; Gnanasekaran, L.; Dutta, K.; Rajendran, S.; Balakrishnan, D.; Soto-Moscoso, M. *Chemosphere* **2022**, *307*, 135957. [Crossref]

[19] Yi, Z.; Yao, J.; Zhu, M.; Chen, H.; Wang, F.; Yuan, Z.; Liu, X. *J. Radioanal. Nucl. Chem*. **2016**, *310*, 505. [Crossref]

[20] Marcellino, S.; Attar, H.; Lièvremont, D.; Lett, M.; Barbier, F.; Lagarde, F. *Anal. Chim. Acta*. **2008**, *629*, 73. [Crossref]

[21] Ciríaco, L.; Santos, D.; Pacheco, M. J.; Lopes, A. *J. Appl. Electrochem*. **2011**, *41*, 577. [Crossref]

[22] dos Anjos, V. E.; Abate, G.; Grassi, M. T. *Quim. Nova* **2010**, *33*, 1307 [Crossref]

[23] Kawak, H. W.; Kim, M. K.; Lee, J. Y.; Yun, H.; Kim, M. H.; Park, Y. H.; Lee, K. H. *Algal Res*. **2015**, *7*, 92. [Crossref]

[24] He, J.; Chen, P. J. *Bioresour. Technol*. **2014**, *160*, 67. [Crossref]

[25] Flores-Chaparro, C. E.; Ruiz, L. F. C.; de la Torre, C. A.; Huerta-Diaz, M. A.; Rangel-Mendez, J. R. *J. Environ. Manage*. **2017**, *193*, 126. [Crossref]

[26] Din, M. I.; Mirza, M. L.; Ata, S.; Athar, M.; Moshin, I. *J. Chem*. **2013**, *528542*, 1. [Crossref]

[27] Kumar, K. Y.; Muralidhara, H. B.; Nayaka, Y. A.; Balasubramanyam, J.; Hanumanthappa, H. *Powder Technol*. **2013**, *246*, 125. [Crossref]

[28] Ubando, A. T.; Marla, A. D. M. A.; Maniquiz-Redillas, C.; Culaba, A. B.; Chen, W.; Chang, J.-S. *J. Hazard. Mater*. **2021**, *402*, 123431. [Crossref]

[29] Sun, F.; Wu, F. C.; Liao, H. Q.; Xing, B. S. *Chem. Eng. J*. **2011**, *171*, 1082. [Crossref]

[30] Madrid, Y.; Barrio-Cordoba, M. E.; Cámara C. *Analyst*. **1998**, *123*, 1593. [Crossref]

[31] Davis, T. A.; Volesky, B.; Mucci, A. *Water Res*. **2003**, *37*, 4311. [Crossref]

[32] Veglio, F.; Beolchini, F. *Hydrometallurgy*. **1997**, *44*, 301. [Crossref]

[33] Volesky, B. *Hydrometallurgy*. **2001**, *59*, 203. [Crossref]

[34] Lodi, A.; Soletto, D.; Solisio, C.; Converti, A. *Chem. Eng. J*. **2008**, *136*, 151. [Crossref]

[35] Gokhale, S.; Lele, S. S. *J. Hazard. Mater*. **2009**, *170*, 735. [Crossref]

[36] Ferreira, L. S.; Rodrigues, M. S.; de Carvalho, J. C. M.; Lodi, A.; Finocchio, E.; Perego, P.; Converti, A. *Chem. Eng. J*. **2011**, *173*, 326. [Crossref]

[37] Fang, L.; Zhou, C.; Cai, P.; Chen, W.; Rong, X.; Dai, K.; Liang, W.; Gu, J. D.; Huang, Q. *J. Hazard. Mater*. **2011**, *190*, 810. [Crossref]

[38] Al-Homaidan, A. A.; Alabdullatif, J. A.; Al-Hazzani, A. A.; Al-Ghanayem, A. A.; Alabbad, A. F. *Saudi J. Biol. Sci*. **2015**, *22*, 795. [Crossref]

[39] Al-Amin, A.; Parvin, F.; Chakraborty, J.; Kim, Y. *Environ. Technol. Rev*. **2021**, *10*, 44. [Crossref]

[40] Wang, J.; Chen, C. *Biotechnol. Adv*. **2009**, *27*, 195. [Crossref]

[42] Son, S. H.; Ahn, J.; Uji, T.; Choi, D.; Park, E.; Hwang, M. S.; Liu, J. R.; Choi, D.; Mikami, K.; Jeong, W. *J. Appl. Phycol*. **2012**, *24*, 79. [Crossref]

[43] Gong, G.; Zhao, J.; Wang, C.; Wei, M.; Dang, T.; Deng, Y.; Sun, J.; Song, S.; Huang, L.; Wang, Z. *Process Biochem*. **2018**, *74*,185. [Crossref]

[44] Şeker, A.; Shahwan, T.; Eroğlu, A. E.; Yılmaz, S.; Demirel, Z.; Dalay, M. C. *J. Hazard. Mater*. **2008**, *154*, 973. [Crossref]

[45] Lukauský, J.: Vonshak, A. *Photosyntetica*. **2000**, *38*, 552. [Crossref]

[46] Akao, P. K.; Cohen-Yaniv, V.; Peretz, R.; Kinel-Tahan, Y.; Yehoshua, Y.; Mamane, H. *Biomass Bioenergy* **2019**, *127*, 105247. [Crossref]

[47] Nithya, K.; Muthukumar, C.; Duraipandiyan, V.; Dhanasekaran, D.; Thajuddin, N. *J. Appl. Pharm. Sci. Res.* **2015**, 7, 117 [Crossref]

[48] Desmorieux, H.; Madiouli, J.; Herraud, C.; Mouaziz, H. *J. Food Eng*. **2010**, *100*, 585. [Crossref]

[49] Gunasundari, E.; Kumar, P. S. *IET Nanobiotechnol*. **2017**, *11*, 317. [Crossref]

[50] Domozych, D. S.; Stewart, K. D.; Mattox, K. *J. Mol. Evol*. **1980**, *15*, 1 [Crossref]

[51] Sing, K. S. W.; Everett, D. H.; Haul, R. A. W.; Moscou, L.; Pierotti, R. A.; Rouquérol, J.; Siemieniewska, T. *Pure & App. Chem*. **1985**, *57*, 603 [Crossref]

[52] Bhatnagar, A.; Jain, A. K. *J. Colloid Interface Sci*. **2005**, *281*, 49. [Crossref]

[53] Benita, S.; Levy, M. Y. *J. Pharm. Sci*. **1993**, 82, 1069. [Crossref]

[54] Venkatesan, S.; Pugazhendy, K.; Sangeetha, D.; Vasantharaja, C.; Prabakaran, S.; Meenambal, M. *Int J. Pharm. Biol. Arch*. **2012**, *3*, 969. [Crossref]

[55] Solomons, T. W. G.; Fryhle, G. B.; Organic Chemistry, 10th ed. New York: John Wiley & Sons, 2011.

[56] Rodrigues, M. S.; Ferreira, L. S.; de Carvalho, J. M. C.; Lodi, A.; Finocchio, E.; Converti, A. *J. Hazard. Mater*. **2012**, *217–218*, 246. [Crossref]

[57] Gagrai, M. K.; Das, C.; Golder, A. K. *Chemosphere* **2013**, *93*, 1366. [Crossref]

[58] Venkatesan, J.; Manivasagan, P.; Kim, S. *Hand. Mar. Microalgae* **2015**, 1. [Crossref]

[59] Ungureanu, G.; Filote, C.; Santos, S. C. R.; Boaventura, R. A. R.; Volf, I.; Botelho, C. M. S. *J. Environ. Chem. Eng*. **2016**, *4*, 3441. [Crossref]

[60] Wu, F.; Sun, F.; Wu, S.; Yan, Y.; Xing, B. *Chem. Eng. J*. **2012**, *183,* 172. [Crossref]

How to cite this article

Dos Anjos, V. E.; da Silva, R. M.; Viana, A. G. *Orbital: Electronic J. Chem*. **2025**, *17*, 186. DOI: http://dx.doi.org/10.17807/orbital.v17i2.20480